ISSN 0021-3640, JETP Letters, 2024, Vol. 119, No. 4, pp. 261–266. © The Author(s), 2024. This article is an open access publication.
Russian Text © The Author(s), 2024, published in Pis'ma v Zhurnal Eksperimental'noi i Teoreticheskoi Fiziki, 2024, Vol. 119, No. 4, pp. 257–262.

OPTICS
AND LASER PHYSICS

Optical Trapping and Moving of Microparticles by the Near Field of Bloch Surface Waves in Polymer Waveguides

V. O. Bessonov[a], A. D. Rozanov[a], and A. A. Fedyanin[a,*]

[a] *Faculty of Physics, Moscow State University, Moscow, 119991 Russia*

**e-mail: fedyanin@nanolab.phys.msu.ru*

Received December 11, 2023; revised December 29, 2023; accepted December 31, 2023

Trapping and movement of microparticles using the near field of waveguide modes enables the realization of stable and compact integrated optical platforms for manipulating, sorting, and studying single microobjects. In this work, the possibility of optical manipulation via Bloch surface waves propagating in polymer waveguides on the surface of a one-dimensional photonic crystal and localizing light at the waveguide surface is studied. Numerical simulation of optical forces acting on a spherical particle from the fundamental waveguide mode of the Bloch surface wave is performed. Using two-photon laser lithography, SU-8 polymer waveguides are fabricated on the surface of a one-dimensional photonic crystal. The movement of a polystyrene microparticle along the waveguide when the Bloch surface wave is excited in it is experimentally demonstrated.

DOI: 10.1134/S0021364024600010

The method for manipulating micro- and nanoobjects via light, called optical tweezers, has been actively used in biology and physics for several decades, in particular to measure forces at the femtonewton level, to study single cells and the viscoelastic properties of media at the microscale [1]. Particle capture occurs due to the appearance of a three-dimensional trap created by gradient forces at the waist of tightly focused laser radiation [2]. In this case, the area of particle manipulation is limited by the spot size and depth of focus of the laser radiation. To move the particles, one must either move the trap or use structured beams which require bulky objective lenses and optical schemes operating in free space [3–5]. In this regard, optical control methods using evanescent fields of surface electromagnetic waves [6–8] and waveguide modes in waveguides of various types [9–12] have been actively developed recently. The concept of integrated optics makes it possible to generate optical forces over long distances limited only by losses in waveguides, as well as to implement the parallel manipulation using a large number of densely packed waveguide systems, making the method significantly cheaper and increasing the flexibility and stability of microobject control.

To achieve effective control, it is necessary to localize the electric field near the surface of the waveguide structure, which is realized in the case of excitation of surface electromagnetic waves. Specifically, the successful trapping and movement of particles by means of surface plasmon-polariton excited both in bare metal films [13, 14] and in metal waveguides [15] have been demonstrated. However, plasmon propagation is always accompanied by Ohmic losses, which reduce the propagation length of plasmons to tens of microns and limit their use in biological applications due to heating. Another type of surface electromagnetic wave is the Bloch surface wave (BSW) that can propagate along the surface of a one-dimensional photonic crystal (PC) in analogy to surface plasmon-polaritons in metal films [16, 17]. Due to the use of dielectric materials, the BSW propagation length can reach centimetres in the visible range [18], and the ability of tailoring the BSW dispersion curve by adjusting the PC thicknesses and materials [19] enables BSW to be excited in a wide spectral range from ultraviolet [20] to terahertz [21]. It was recently shown that BSW can travel along a polymer stripe on the PC surface, acting as a waveguide [22–25]. As a result, a variety of elements of two-dimensional polymer integrated optics based on BSW have been implemented [26, 27], including interferometers [28], input/output coupling elements [29], and microlasers [30]. BSW can also be used to optically trap, move and aggregate particles [8, 31–33]. However, in these works, BSW was excited on the bare PC surface and had a typical beam width of several tens of microns.

In this work, we study the possibility of trapping and moving a microparticle via BSW propagating along a micron-wide polymer waveguide on the PC surface. Numerical simulation of the forces acting on the particle from the side of BSW is performed, depending on the waveguide parameters. Polymer waveguides are fabricated on the PC surface using two-photon laser lithography, and the motion of a 1 μm diameter polystyrene particle along the wave-

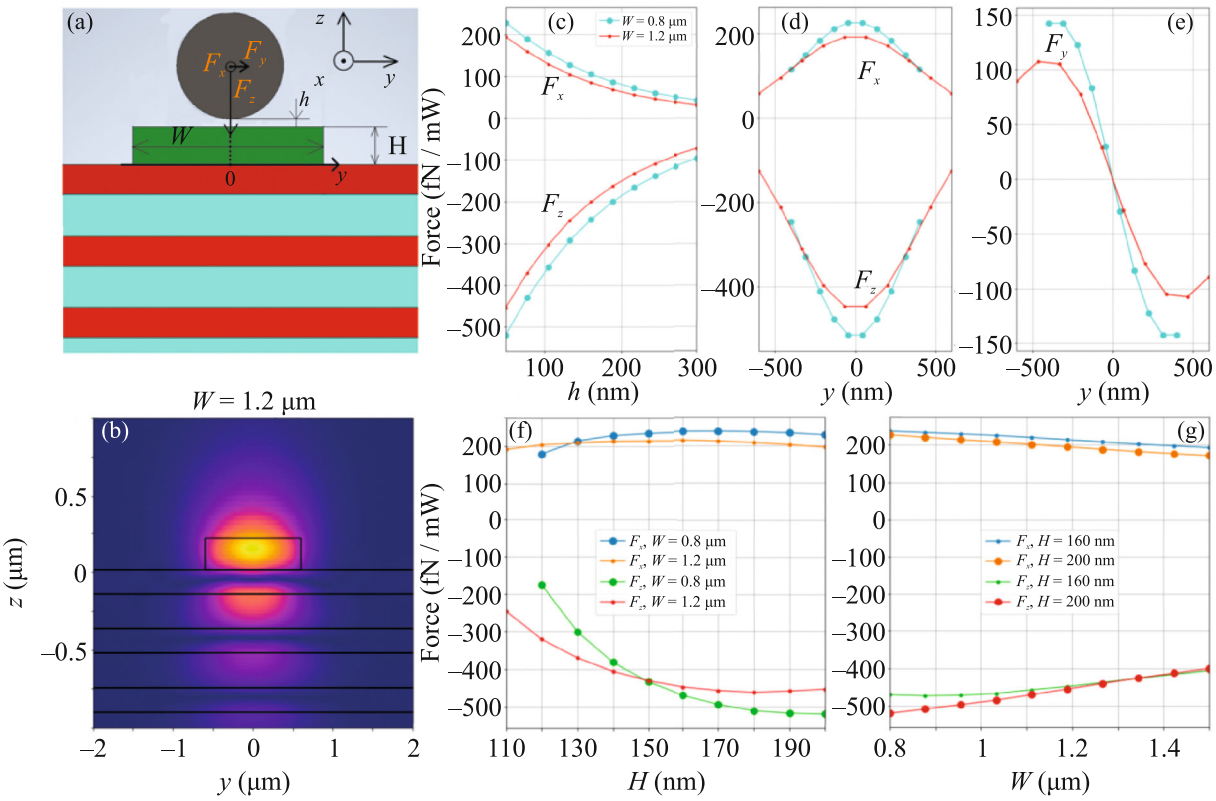

Fig. 1. (Color online) Numerical simulation. (a) Schematic of the system under study. A spherical particle is located in water above a waveguide situated on the surface of a one-dimensional photonic crystal. BSW waveguide modes propagate along the x-axis. (b) Electric field distribution in the TE_{00} BSW mode propagating in a waveguide with the height $H = 180$ nm and the width $W = 1.2$ μm. (c, d, e) Dependences of the projections of the force acting on the particle from the TE_{00} BSW mode on the gap h between the particle and the waveguide and the particle position relative to the waveguide center at $h = 50$ nm. (f, g) Dependences of the force projections on the height and width of the waveguide at the gap value $h = 50$ nm.

guide is demonstrated when the fundamental BSW mode is excited.

Numerical simulations and experiments were carried out at a wavelength of 638 nm. The scheme of the system under study is shown in Fig. 1a. A spherical polystyrene particle with a refractive index of 1.59 and a diameter of 1 μm is located in a water medium (refractive index is 1.333) at a distance h from a waveguide. The waveguide made of SU-8 polymer with a refractive index of 1.58 supports the propagation of the fundamental BSW mode along the x-axis. The one-dimensional photonic crystal consists of four pairs of 223-nm-thick SiO_2 layers and 156-nm-thick Ta_2O_5 layers with refractive indices of 1.478 and 2.135, respectively. The PC parameters are calculated so that BSW cannot occur on the bare surface and is excited only in the waveguide. For these PC parameters, the waveguide is single-mode in the width W range from 0.8 to 1.2 μm and height H range from 110 to 200 nm. In this case, the effective refractive index of the fundamental TE_{00} BSW mode varies between 1.34 and 1.37, which is very close to the refractive index of water and ensures the BSW field localization at the top of the waveguide, as well as effective field penetration into the water medium above the waveguide (Fig. 1b).

Numerical simulations were performed by the finite difference time domain method using the Lumerical FDTD Solutions software. The values of the force acting on the particle from the BSW field were calculated by integrating the components of the Maxwell stress tensor [34]. Figure 1 shows the dependence of the force projections on the particle position relative to the 180 nm high waveguide, normalized to the power of the BSW radiation. It can be seen from Fig. 1c that the gradient force F_z increases as the gap between the particle and the waveguide decreases, thereby pushing the particle towards the waveguide. The propulsion force F_x also increases with decreasing gap, while its typical values are an order of magnitude larger than for the classical waveguide mode in an SU-8 waveguide on a quartz substrate [9]. The maximum values of the forces F_x and F_z are reached when the particle is positioned in the center of the waveguide (see Fig. 1d), while the force F_y acting across the

waveguide vanishes. Figure 1e demonstrates that when the particle is shifted from the center of the waveguide, F_y increases, pulling the particle back toward the center and, together with the force F_z, ensuring stable trapping of the particle. In all cases, a decrease in the maximum force value is observed as the waveguide width increases, which is associated with a decrease of the depth of BSW field penetration into the external environment. The calculation also shows that the force F_z decreases more than 2 times as the waveguide height H decreases from 150 to 110 nm and varies slightly in the height range from 150 to 200 nm, while F_x is almost independent of the waveguide height and varies within 10% (Fig. 1f). The force value also weakly depends on the width of the waveguide, decreasing monotonically by 20% with an increase in width from 0.8 to 1.5 μm. Therefore, in an experiment on particle motion, it makes sense to use waveguides with a height of at least 150 nm and a width corresponding to the single-mode regime. Numerical estimates of the propagation length of the TE_{00} BSW mode range from 100 μm for the waveguide with H = 150 nm and W = 0.8 μm to 370 μm for the waveguide with H = 200 nm and W = 1.2 μm.

The photonic crystal samples were fabricated on a 170-μm-thick glass (BK-7) substrate using magnetron sputtering. Waveguide structures on the PC surface were fabricated by two-photon laser lithography in thin films of SU-8 2015 photoresist (Microchem), the thickness of which determined the height of the waveguides and was chosen in the range from 150 to 200 nm. The method of producing samples is described in detail in [28, 35, 36]. The waveguide structure (Fig. 2a) consisted of an 80-μm-long coupling triangle with a 26-μm base, onto which the pump radiation is focused, and a straight waveguide whose length varied from 95 to 140 μm. Using adhesive tape and a 150-μm-thick cover glass, a cell was formed around the waveguides and filled with an aqueous solution of the following composition: sodium dodecyl sulphate—surfactant—with a concentration of 0.01 mM to prevent the adhesion of microparticles to the surface of the waveguide and PC; sodium azide at a concentration of 0.02% to prevent the formation of bacteria in the solution; spherical polystyrene particles with a diameter of 1 μm and a concentration of 1 μg/mL. The excitation of BSW modes in the waveguides was implemented in the Kretschmann geometry (Fig. 2b) by focusing TE-polarized radiation in the coupling triangle into a spot 20 × 50 μm in size. The cell was placed on a glass prism through an immersion oil. The radiation of a continuous diode laser with a wavelength of 638 nm was directed onto the sample from the prizm side at an angle of incidence, which could be adjusted in the range from 58° to 70°. Visualization of the sample and of the laser radiation scattered by the waveguide and the particles was performed using a water immersion objective lens (numerical aperture of 1.2, focal length of 3 mm) mounted on the side of the cover glass and a CMOS camera. The same objective lens was used to form the optical trap at a wavelength of 1064 nm, which optically trapped single microparticles and transferred them to the waveguide surface.

To excite BSW in the Kretschmann geometry, it is necessary to fulfill the phase-matching condition $n_{pr}\sin\phi = n_{eff}^{BSW}$ [29], where n_{eff}^{BSW} is the effective refractive index of the BSW mode and n_{pr} = 1.516 is the refractive index of the prism material. Since the mode effective refractive index must be higher than the refractive index of water, the angle of incidence of radiation on PC must exceed the angle of total internal reflection at the prism/water interface, which is 61.5°. On the other hand, for efficient transfer of radiation energy into BSW, the angular beam width should be comparable to the angular width of the BSW resonance, which is determined by the BSW propagation length [37, 38]. Consequently, the pump beam size along the waveguide should be comparable to the BSW propagation length of 100–400 μm for the fabricated waveguides. In the experiment, we used a beam with a diameter of 20 μm, stretched along the waveguide to 50 μm due to oblique incidence, and its divergence was 1.45°. As a result, the low beam divergence enabled selective excitation of BSW waveguide modes by positioning the beam directly on the waveguide and adjusting the incidence angle of radiation in accordance with the phase-matching condition. Figure 3a shows an example of mode composition of the waveguide with dimensions H = 180 nm and W = 1.2 μm. The pump spot was positioned on the waveguide to the right of the triangle, and the signal scattered on the waveguide end was measured depending on the angle of incidence of radiation on the sample. In the graph in Fig. 3b, two maxima are visible at angles of incidence of 62.6° and 65°, corresponding to the excitation of two different BSW modes in the waveguide. Using the phase-matching formula, it is possible to obtain the values of the effective refractive indices of the modes, which are $n_{eff}^{TE_{00}} = 1.373$ and $n_{eff}^{TE_{01}} = 1.345$. According to calculations, $n_{eff}^{TE_{00}} = 1.371$ and $n_{eff}^{TE_{01}} = 1.333$ for the waveguide with the above parameters. Thus, it can be concluded that TE_{00} and TE_{01} BSW modes are excited in the experiment, but their effective refractive indices exceed the calculated ones. This may be associated with errors in the size of waveguides that emerge during their fabrication, as well as with the formation of the tens of nanometers thick surfactant film on the waveguide surface, since the surfactant concentration slightly exceeds the critical concentration for micelle formation [39]. For example, increasing the waveguide width by 100 nm and height by 20 nm leads to values of the effective refractive indices of the BSW

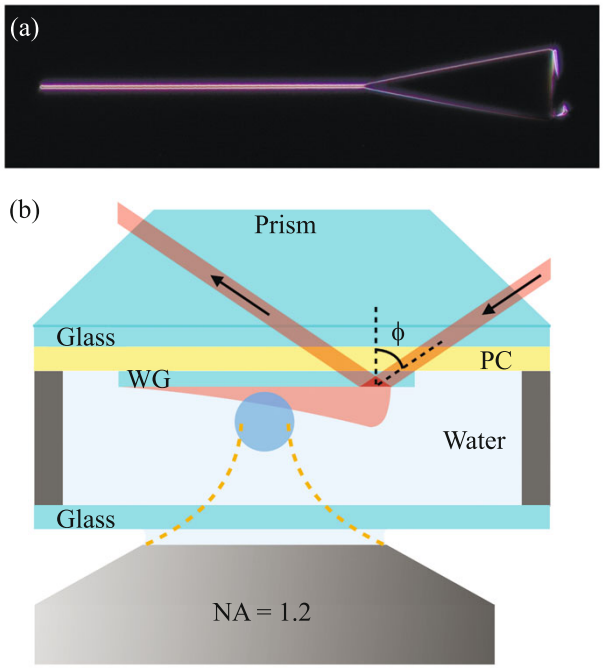

Fig. 2. (Color online) Experimental sample and setup. (a) Dark-field microscopy image of the waveguide structure printed on the PC surface. (b) Scheme of the experiment: (PC) photonic crystal and (WG) waveguide. Yellow dashed curves depict the beam of optical tweezers used to bring the particle to the waveguide.

modes $n_{\text{eff}}^{TE_{00}} = 1.378$ and $n_{\text{eff}}^{TE_{01}} = 1.342$ close to those obtained in the experiment.

In the experiment on the trapping and movement of particles by the BSW field, it is important that only TE_{00} mode is excited in the waveguides. When multiple modes propagate simultaneously, multimode interference occurs, leading to a change in the BSW near-field distribution depending on the coordinate along the waveguide [28]. In this case, the uniform motion of the particle along the waveguide is most likely impossible, and the problem should be considered separately. The experiment was therefore carried out for the waveguides with a minimum design height $H = 150$ nm and width $W = 0.8$ μm, in which the single-mode regime is maintained even in the presence of the above-mentioned size additions. By positioning the pump spot on the waveguide, it was found that only one mode with an effective refractive index $n_{\text{eff}} = 1.339$ is supported by the waveguide. The pump spot then moved to the triangle, where BSWs were generated from the entire spot area and focused into the waveguide due to reflections from the triangle edges. Using optical tweezers, arbitrary particle was trapped in the field of view of the objective lens and transferred to the waveguide. The particle was placed at a distance of 5 μm from the triangle/waveguide junction, after which the trap was turned off. Figure 3c shows the images of the scattered pump radiation taken at regular intervals during the first 12 seconds after the trap was turned off. It can be seen that BSW excited in the waveguide ensures stable movement of the particle strictly along the waveguide. In total, the particle travelled for 66 seconds, moving 65 μm before being displaced from the waveguide due to thermal motion. The average velocity in the first few seconds was 2.2 μm/s and gradually decreased as the particle moved away from the beginning of the waveguide because of BSW attenuation. Applying Stokes' law with a correction for the viscous friction force associated with additional hydrodynamic resistance near the surface [40], the propulsion force can be estimated from the velocity of the particle, which was $F_x = 47$ fN for the estimated distance $h = 50$ nm between the particle and the waveguide. Based on the calculations pre-

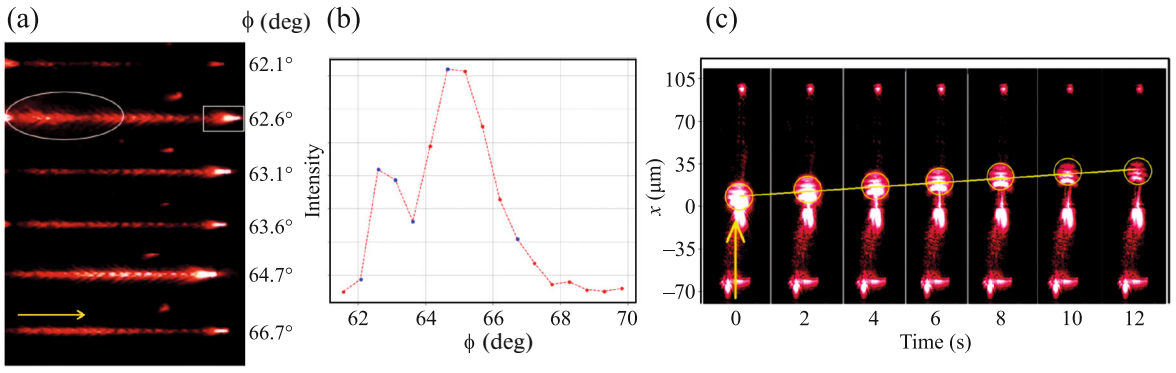

Fig. 3. (Color online) Experimental results. (a) Images of scattering of BSW excited in the waveguide with $H = 180$ nm and $W = 1.2$ μm at various angles of incidence. The white ellipse indicates the position and size of the pump spot. The white rectangle indicates the area from which the scattered radiation is detected. (b) Intensity of radiation scattered at the end of the waveguide as a function of the angle of incidence. (c) Series of images of a particle above the waveguide with $H = 150$ nm and $W = 0.8$ μm, taken with an interval of 2 seconds. Yellow circles indicate a spot of light scattered by the particle moving along the waveguide under the action of the BSW field.

sented in Fig. 1, the corresponding power of the BSW mode can be estimated as 0.2 mW.

In summary, the stable trapping and moving of a microparticle along a polymer waveguide on the surface of a one-dimensional photonic crystal are demonstrated when the fundamental mode of the Bloch surface wave is excited in the waveguide. It is numerically shown that at a mode radiation power of 1 mW, the typical value of the propulsion force of the Bloch surface wave is from 100 to 200 fN for a 1 μm polystyrene spherical particle, which is an order of magnitude larger than in the case of conventional waveguide mode in a polymer waveguide on a quartz substrate. The system under study is experimentally implemented and the movement of the microparticle along a micron-width waveguide at a velocity of 2.2 μm/s is demonstrated.

ACKNOWLEDGMENTS

We are grateful to D.A. Shilkin and K.R. Safronov for help in carrying out experiments and for useful discussions.

FUNDING

This work was supported by the Russian Science Foundation, project no. 22-22-00874.

CONFLICT OF INTEREST

The authors of this work declare that they have no conflicts of interest.

OPEN ACCESS

REFERENCES

1. G. Volpe, O. M. Marago, H. Rubinsztein-Dunlop, et al., J. Phys. Photon. **5**, 022501 (2023).
2. A. Ashkin, J. M. Dziedzic, J. E. Bjorkholm, and S. Chu, Opt. Lett. **11**, 288 (1986).
3. Yu. V. Pichugina and A. S. Machikhin, Fotonika **14**, 254 (2020).
4. S. P. Kotova, N. N. Losevskii, A. M. Maiorova, and S. A. Samagin, Bull. Russ. Acad. Sci.: Phys. **87**, 1767 (2023).
5. A. B. Stilgoe, T. A. Nieminen, and H. Rubinsztein-Dunlop, Nat. Photon. **16**, 346 (2022).
6. M. L. Juan, M. Righini, and R. Quidant, Nat. Photon. **5**, 349 (2011).
7. Y. Ren, Q. Chen, M. He, X. Zhang, H. Qi, and Y. Yan, ACS Nano **15**, 6105 (2021).
8. D. A. Shilkin, E. V. Lyubin, I. V. Soboleva, and A. A. Fedyanin, Opt. Lett. **40**, 4883 (2015).
9. B. S. Schmidt, A. H. J. Yang, D. Erickson, and M. Lipson, Opt. Express **15**, 14322 (2007).
10. A. H. J. Yang, S. D. Moore, B. S. Schmidt, M. Klug, M. Lipson, and D. Erickson, Nature (London, U.K.) **457**, 71 (2009).
11. S. Gaugiran, S. Gétin, J. M. Fedeli, G. Colas, A. Fuchs, F. Chatelain, and J. Dérouard, Opt. Express **13**, 6956 (2005).
12. S. Lin, E. Schonbrun, and K. Crozier, Nano Lett. **10**, 2408 (2010).
13. V. Garcés-Chávez, R. Quidant, P. J. Reece, G. Badenes, L. Torner, and K. Dholakia, Phys. Rev. B **73**, 085417 (2006).
14. Y. Zhang, C. Min, X. Dou, X. Wang, H. P. Urbach, M. G. Somekh, and X. Yuan, Light Sci. Appl. **10**, 59 (2021).
15. K. Wang, E. Schonbrun, P. Steinvurzel, and K. B. Crozier, Nano Lett. **10**, 3506 (2010).
16. P. Yeh, A. Yariv, and A. Y. Cho, Appl. Phys. Lett. **32**, 104 (1978).
17. A. Sinibaldi, N. Danz, E. Descrovi, P. Munzert, U. Schulz, F. Sonntag, L. Dominici, and F. Michelotti, Sens. Actuators, B **174**, 292 (2012).
18. B. Vosoughi Lahijani, N. Descharmes, R. Barbey, G. D. Osowiecki, V. J. Wittwer, O. Razskazovskaya, T. Südmeyer, and H. P. Herzig, Adv. Opt. Mater. **10**, 2102854 (2022).
19. K. R. Safronov, V. O. Bessonov, and A. A. Fedyanin, JETP Lett. **114**, 321 (2021).
20. R. Badugu, J. Mao, S. Blair, D. Zhang, E. Descrovi, A. Angelini, Y. Huo, and J. R. Lakowicz, J. Phys. Chem. C **120**, 28727 (2016).
21. C. Zhang, Q. Liu, X. Peng, Z. Ouyang, and S. Shen, Nanophotonics **10**, 3879 (2021).
22. E. Descrovi, T. Sfez, M. Quaglio, D. Brunazzo, L. Dominici, F. Michelotti, H. P. Herzig, O. J. Martin, and F. Giorgis, Nano Lett. **10**, 2087 (2010).
23. T. Sfez, E. Descrovi, L. Yu, D. Brunazzo, M. Quaglio, L. Dominici, W. Nakagawa, F. Michelotti, F. Giorgis, O. J. F. Martin, and H. P. Herzig, J. Opt. Soc. Am. B **27**, 1617 (2010).
24. D. A. Shilkin, K. R. Safronov, A. D. Rozanov, V. O. Bessonov, and A. A. Fedyanin, Mosc. Univ. Phys. Bull. **78**, 179 (2023).
25. E. A. Bezus, Izv. Akad. Nauk, Ser. Fiz. **86**, 6 (2022).
26. L. Yu, E. Barakat, T. Sfez, L. Hvozdara, J. di Francesco, and H. P. Herzig, Light Sci. Appl. **3**, e124 (2014).
27. R. Wang, H. Xia, D. Zhang, J. Chen, L. Zhu, Y. Wang, E. Yang, T. Zang, X. Wen, G. Zou, P. Wang, H. Ming,

R. Badugu, and J. R. Lakowicz, Nat. Commun. **8**, 14330 (2017).

28. K. R. Safronov, D. N. Gulkin, I. M. Antropov, K. A. Abrashitova, V. O. Bessonov, and A. A. Fedyanin, ACS Nano **14**, 10428 (2020).
29. K. R. Safronov, V. O. Bessonov, D. V. Akhremenkov, M. A. Sirotin, M. N. Romodina, E. V. Lyubin, I. V. Soboleva, and A. A. Fedyanin, Laser Photon. Rev. **16**, 2100542 (2022).
30. Y.-C. Lee, Y.-L. Ho, B.-W. Lin, M.-H. Chen, D. Xing, H. Daiguji, and J.-J. Delaunay, Nat. Commun. **14**, 6458 (2023).
31. D. A. Shilkin, E. V. Lyubin, and A. A. Fedyanin, ACS Photon. **9**, 211 (2022).
32. F. Lu, L. Gong, Y. Kuai, X. Tang, Y. Xiang, P. Wang, and D. Zhang, Photon. Res. **10**, 14 (2022).
33. D. A. Shilkin and A. A. Fedyanin, JETP Lett. **115**, 136 (2022).
34. D. A. Shilkin, E. V. Lyubin, M. R. Shcherbakov, M. Lapine, and A. A. Fedyanin, ACS Photon. **4**, 2312 (2017).
35. K. A. Abrashitova, D. N. Gulkin, K. R. Safronov, N. G. Kokareva, I. M. Antropov, V. O. Bessonov, and A. A. Fedyanin, Appl. Sci. (Switzerland) **8**, 63 (2018).
36. M. D. Aparin, T. G. Baluyan, M. I. Sharipova, M. A. Sirotin, E. V. Lyubin, I. V. Soboleva, V. O. Bessonov, and A. A. Fedyanin, Bull. Russ. Acad. Sci.: Phys. **87**, 710 (2023).
37. I. V. Soboleva, V. V. Moskalenko, and A. A. Fedyanin, Phys. Rev. Lett. **108**, 123901 (2012).
38. F. I. Baida and M.-P. Bernal, Commun. Phys. **3**, 86 (2020).
39. A. Dominguez, A. Fernandez, N. Gonzalez, E. Iglesias, and L. Montenegro, J. Chem. Educ. **74**, 1227 (1997).
40. Y. Kazoe and M. Yoda, Appl. Phys. Lett. **99**, 124104 (2011).

Translated by the authors